Electronic Supplementary Material (ESI) for Physical Chemistry Chemical Physics.

Supporting Information for

Charge transport parameters for carbon based nanohoops and donor-acceptor derivatives

Sofia Canola [†‡], Christina Graham [†§‖], Ángel José Pérez-Jiménez [§], Juan-Carlos Sancho-García [§] and Fabrizia Negri [†‡]**

† Università di Bologna, Dipartimento di Chimica 'G. Ciamician', Via F. Selmi, 2, 40126.

‡ INSTM, UdR Bologna, Italy.

§ Department of Physical Chemistry, University of Alicante, 03080 Alicante, Spain.

‖ Institute of Photonic Sciences (ICFO), Spain.

Table S1. Absolute energies of the pristine and oxidized/reduced forms, of [6]CPP , [8]CPP , [10]CPP and DMA[8]CPP, employed to evaluate the intramolecular reorganization energies according to the AP method. B3LYP/6-31G* level of theory in vacuo unless specified.

Pristine-oxidized

	$(E_p^{geo\text{-}p})$	$(E_o^{geo\text{-}o})$	$(E_p^{geo\text{-}o})$	$(E_o^{geo\text{-}p})$
[6]CPP	-1386.188622	-1385.971772	-1386.181967	-1385.965130
[8]CPP	-1848.342797	-1848.123995	-1848.338080	-1848.119203
[12]CPP	-2772.612970	-2772.395385	-2772.609876	-2772.392197
trans-DMA[8]CPP	-1959.761901	-1959.385059	-1959.756134	-1959.378882
cis-DMA[8]CPP	-1959.765271	-1959.387221	-1959.759190	-1959.381185
cis-DMA[8]CPP[a]	-1960.174084	-1959.974113	-1960.168345	-1959.968403

Pristine-reduced

	$(E_p^{geo\text{-}p})$	$(E_r^{geo\text{-}r})$	$(E_p^{geo\text{-}r})$	$(E_r^{geo\text{-}p})$
[6]CPP	1836.188622	-1386.218763	-1386.181737	-1386.211656
[8]CPP	-1848.342797	-1848.375287	-1848.337432	-1848.369659
[12]CPP	-2772.612970	-2772.650136	-2772.608969	-2772.645906
trans-DMA[8]CPP	-1959.761901	-1960.005432	-1959.757850	-1960.001579
cis-DMA[8]CPP	-1959.765271	-1960.006773	-1960.760718	-1959.002660
cis-DMA[8]CPP[a]	-1960.174084	-1960.292209	-196.168550	-1960.286809

[a]Calculations carried out in acetonitrile described with the CPCM model and intra-molecular dispersion interactions with the D3(BJ) correction term.

Table S2. Frontier orbital energies and their energy gap of [8]CPP and DMA[8]CPP computed at the B3LYP/6-31G* optimized structures of the pristine species.

	E(*HOMO*) / *eV*	*E*(*LUMO*) / *eV*	*ΔE(H-L) geo-pristine*
[6]CPP	-4.91	-1.78	3.13
[8]CPP	-5.10	-1.71	3.39
[12]CPP	-5.25	-1.64	3.61
trans-DMA[8]CPP	-9.33	-7.54	1.79
cis- DMA[8]CPP	-9.35	-7.47	1.87
cis- DMA[8]CPP [a]	-5.70	-2.95	2.75

[a] Calculations carried out in acetonitrile described with the CPCM model and intra-molecular dispersion interactions with the D3(BJ) correction term.

Table S3 Adiabatic Potential (AP) intramolecular reorganization energies (eV) computed for the investigated nanohoops at B3LYP/6-31G* level of theory in vacuo unless specified.

p-type charge transport

	$\lambda_i^{p(AP)}$ [a]	$\lambda_i^{o(AP)}$ [b]	λ_i^{AP}	λ_i^{AP} [d]
[6]CPP	0.181	0.181	0.362	0.380
[8]CPP	0.128	0.130	0.259	0.281
[12]CPP	0.084	0.087	0.171	0.191
trans-DMA[8]CPP	0.157	0.167	0.324	-
cis-DMA[8]CPP	0.165	0.164	0.330	-
cis-DMA[8]CPP[e]	0.156	0.155	0.311	-

n-type charge transport

	$\lambda_i^{p(AP)}$ a	$\lambda_i^{r(AP)}$ c	λ_i^{AP}	λ_i^{APd}
[6]CPP	0.187	0.193	0.381	0.373
[8]CPP	0.146	0.153	0.299	0.302
[12]CPP	0.109	0.115	0.224	0.233
trans-DMA[8]CPP	0.112	0.104	0.216	-
cis-DMA[8]CPP	0.124	0.112	0.236	-
cis-DMA[8]CPP[e]	0.151	0.147	0.298	-

[a] Contribution from the pristine system, computed according to the AP method. [b] Contribution from the oxidized form, computed according to the AP method. [c] Contribution from the reduced form, computed according to the AP method. [d] from ref. [1], from B3LYP/6-31+G* calculations. [e] Calculations carried out in acetonitrile described with the CPCM model and intra-molecular dispersion interactions with the D3(BJ) correction term.

Table S4 . Center of mass distances and vectorial components for the dimers extracted from the crystal structure of [6]CPP, [8]CPP, [12]CPP and DMA[8]CPP and whose electronic couplings have been computed**.**

[6]CPP

Name	Intermol dist. [Å]	d*x* [Å]	d*y* [Å]	d*z* [Å]
D01a	7.6388	-1.5846	-5.1560	5.4089
D01b	7.6388	1.5846	5.1560	-5.4089
D01c	7.6388	-1.5846	5.1560	5.4089
D01d	7.6388	1.5846	-5.1560	-5.4089
D02a	10.3120	0.0000	-10.3120	0.0000
D02b	10.3120	0.0000	10.3120	0.0000
D03a	11.1772	11.1772	0.0000	0.0000
D03b	11.1772	-11.1772	0.0000	0.0000
D04a	12.1597	9.5926	-5.1560	5.4089
D04b	12.1597	9.5926	5.1560	5.4089
D04c	12.1597	-9.5926	-5.1560	-5.4089
D04d	12.1597	-9.5926	5.1560	-5.4089
D05a	15.2075	11.1772	-10.3120	0.0000
D05b	15.2075	11.1772	10.3120	0.0000
D05c	15.2075	-11.1772	-10.3120	0.0000
D05d	15.2075	-11.1772	10.3120	0.0000

[8]CPP

Name	Intermol dist. [Å]	d*x* [Å]	d*y* [Å]	d*z* [Å]
D01a	8.0103	0.0000	-8.0103	0.0000
D01b	8.0103	0.0000	8.0103	0.0000
D02a	10.8835	-3.9007	-4.0051	-9.3378
D02b	10.8835	-3.9007	4.0051	-9.3378
D02c	10.8835	3.9007	-4.0051	9.3378
D02d	10.8835	3.9007	4.0051	9.3378
D03a	12.9325	-12.9325	0.0000	0.0000
D03b	12.9325	12.9325	0.0000	0.0000
D04a	13.5944	-9.0318	-4.0051	9.3378

D04b	13.5944	-9.0318	4.0051	9.3378
D04c	13.5944	9.0318	-4.0051	-9.3378
D04d	13.5944	9.0318	4.0051	-9.3378
D05a	15.2123	-12.9325	-8.0103	0.0000
D05b	15.2123	-12.9325	8.0103	0.0000
D05c	15.2123	12.9325	-8.0103	0.0000
D05d	15.2123	12.9325	8.0103	0.0000

[12]CPP

Name	Intermol dist. [Å]	d*x* [Å]	d*y* [Å]	d*z* [Å]
D01a	8.1878	0.0000	-8.1878	0.0000
D01b	8.1878	0.0000	8.1878	0.0000
D02a	12.5231	3.2933	-4.0939	-11,3676
D02b	12.5231	-3.2933	-4.0939	11,3676
D02c	12.5231	3.2933	4.0939	-11,3676
D02d	12.5231	-3.2933	4.0939	11,3676
D03a	18.5827	18.5827	0.0000	0.0000
D03b	18.5827	-18.5827	0.0000	0.0000
D04a	19.4871	-15.2894	-4.0939	-1.3676
D04b	19.4871	-15.2894	4.0939	-1.3676
D04c	19.4871	15.2894	-4.0939	1.3676
D04d	19.4871	15.2894	4.0939	1.3676
D05a	20.3066	-18.5827	-8.1878	0.0000
D05b	20.3066	18.5827	-8.1878	0.0000
D05c	20.3066	18.5827	8.1878	0.0000
D05d	20.3066	-18.5827	8.1878	0.0000

DMA[8]CPP

Name	Intermol dist. [Å]	d*x* [Å]	d*y* [Å]	d*z* [Å]
D01a	10.3840	0.0000	-10.3840	0.0000
D01b	10.3840	0.0000	10.3840	0.0000
D02a	13.8313	11.9739	-5.1920	-4.5797
D02b	13.8313	11.9739	5.1920	4.5797
D03a	13.9330	1.5185	0.0339	-13.8500
D03b	13.9330	-1.5185	-0.0339	13.8500

D04a	14.5269	-12.7711	-5.1920	-4.5797
D04b	14.5269	-12.7711	5.1920	-4.5797
D05	14.8949	10.4553	-5.1581	9.2703
D06	14.9185	10.4553	5.2259	9.2703

Table S5. Parameters employed for the calculation of MLJ and SO rate constants: effective frequency ω_{eff} and associated Huang-Rhys factor S_{eff}; spectral overlap *SO* employed in the evaluation of charge transfer rate constants of [8]CPP and DMA[8]CPP at B3LYP/6-31G* level of theory.

		MLJ					*SO*
		ω_{eff} [a] (cm^{-1})	S_{eff} [a]	λ_i [a] (eV)	λ_{class} [b] (eV)	Total λ_{class} [c] (eV)	*SO* (eV^{-1})
[8]CPP	*p*-type	875	1.153	0.125	0.144	0.154	0.547
	n-type	1127	1.187	0.166	0.154	0.164	0.424
DMA[8]CPP	*p*-type[b]	794	2.537	0.250	0.084	0.094	0.256
	n-type	656	2.102	0.171	0.096	0.106	0.600

[a] Only frequencies above 200 cm^{-1} were considered in the calculation of the effective quantum-chemical parameters. [b] λ_{class} contribution to the intra-molecular reorganization energy from classical intra-molecular vibrational modes. [c] A value of λ_s of 0.01 eV was assumed based on recent estimates.

Table S6 Electronic couplings V_{ij} (B3LYP/6-31G* level of theory) and charge transfer rate constants k_{CT} computed for the different charge hopping paths in the crystal of [8]CPP.

[8]CPP – *p*-type

dimer	distance (Å)	V_{ij}^{HOMO} (meV)	k_{CT} (ps^{-1})		
			Marcus	*MLJ*	*Spectral overlap* [a]
D01	8.0103	1	0.00	0.01	0.01
D02	10.8835	8	0.15	0.22	0.36
D03	12.9325	16	0.55	0.84	1.36
D04	13.5944	6	0.07	0.11	0.17
D05a	15.2123	5	0.05	0.07	0.11

[8]CPP – *n*-type

dimer	distance (Å)	V_{ij}^{LUMO} (meV)	k_{CT} (ps^{-1})		
			Marcus	*MLJ*	*Spectral overlap* [a]
D01	8.0103	3	0.01	0.03	0.05
D02	10.8835	11	0.16	0.34	0.52
D03	12.9325	10	0.13	0.29	0.44
D04	13.5944	16	0.32	0.70	1.07
D05a	15.2123	7	0.06	0.14	0.20

[a] Parameters employed for spectra simulation: broadening with Gaussian function having half width at half maximum (hwhm) of 320 cm^{-1} (0.04 eV), temperature = 300 K.

Table S7 Electronic couplings V_{ij} (B3LYP/6-31G* level of theory) and charge transfer rate constants k_{CT} computed for the different charge hopping paths in the crystal of DMA[8]CPP.

DMA[8]CPP – *p*-type

dimer	distance (Å)	V_{ij}^{HOMO} (meV)	k_{CT} (ps^{-1})		
			Marcus	*MLJ*	*Spectral overlap*
D01	10.3840	0	0.00	0.00	0.00
D02	13.8313	9	0.08	0.16	0.20
D03	13.9330	0	0.00	0.00	0.00
D04	14.5269	0	0.00	0.00	0.00
D05	14.8949	113	13.1	25.5	31.3
D06	14.9185	0	0.00	0.00	0.00

DMA[8]CPP – *n*-type

dimer	distance (Å)	V_{ij}^{LUMO} (meV)	k_{CT} (ps^{-1})		
			Marcus	*MLJ*	*Spectral overlap*
D01	10.3840	0	0.00	0.00	0.00
D02	13.8313	3	0.02	0.03	0.05
D03	13.9330	0	0.00	0.00	0.00
D04	14.5269	3	0.02	0.03	0.06
D05	14.8949	2	0.01	0.01	0.03
D06	14.9185	0	0.00	0.00	0.00

[a] Parameters employed for spectra simulation: broadening with Gaussian function having half width at half maximum (hwhm) of 320 cm^{-1} (0.04 eV), temperature = 300 K.

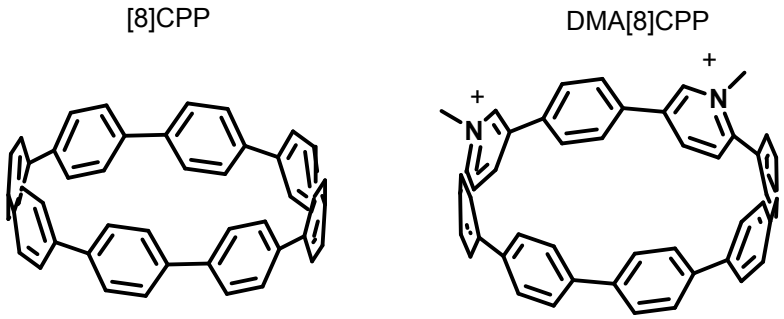

Figure S1. Chemical structure of [8]CPP and its donor-acceptor derivative DMA[8]CPP

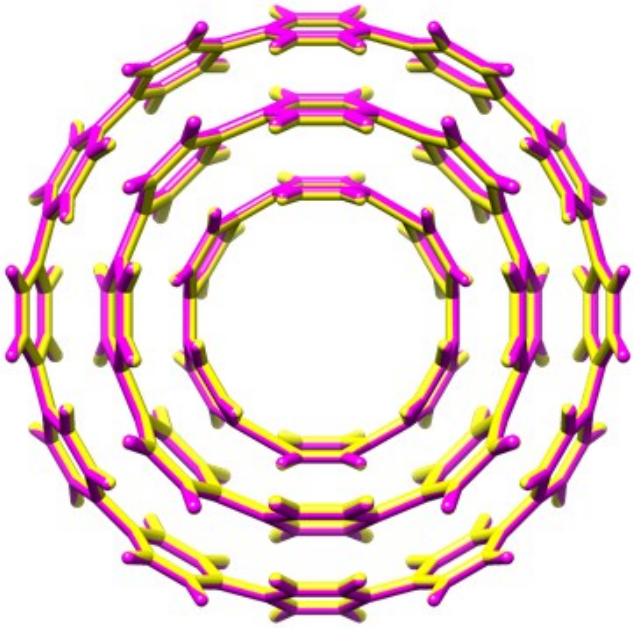

Figure S2. Comparison between the equilibrium structure of the reduced form (magenta) of [n]CPP and the oxidized form (yellow). From outside to inside [12]CPP, [8]CPP and [6]CPP. From B3LYP/6-31G* calculations. The three structures are not on the same scale. They were rescaled to fit one inside the other.

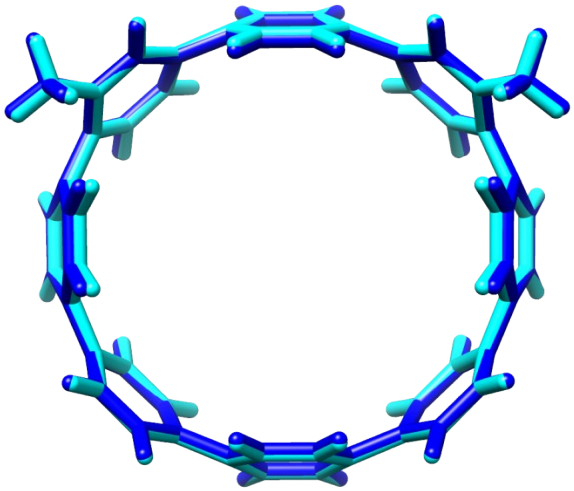

Figure. S3. Comparison between the equilibrium structure of the pristine form of DMA[8]CPP from B3LYP/6-31G* calculations in vacuo (blue) and in acetonitrile described with the CPCM model supplemented with intra-molecular dispersion interactions described with the D3(BJ) correction term (cyan).

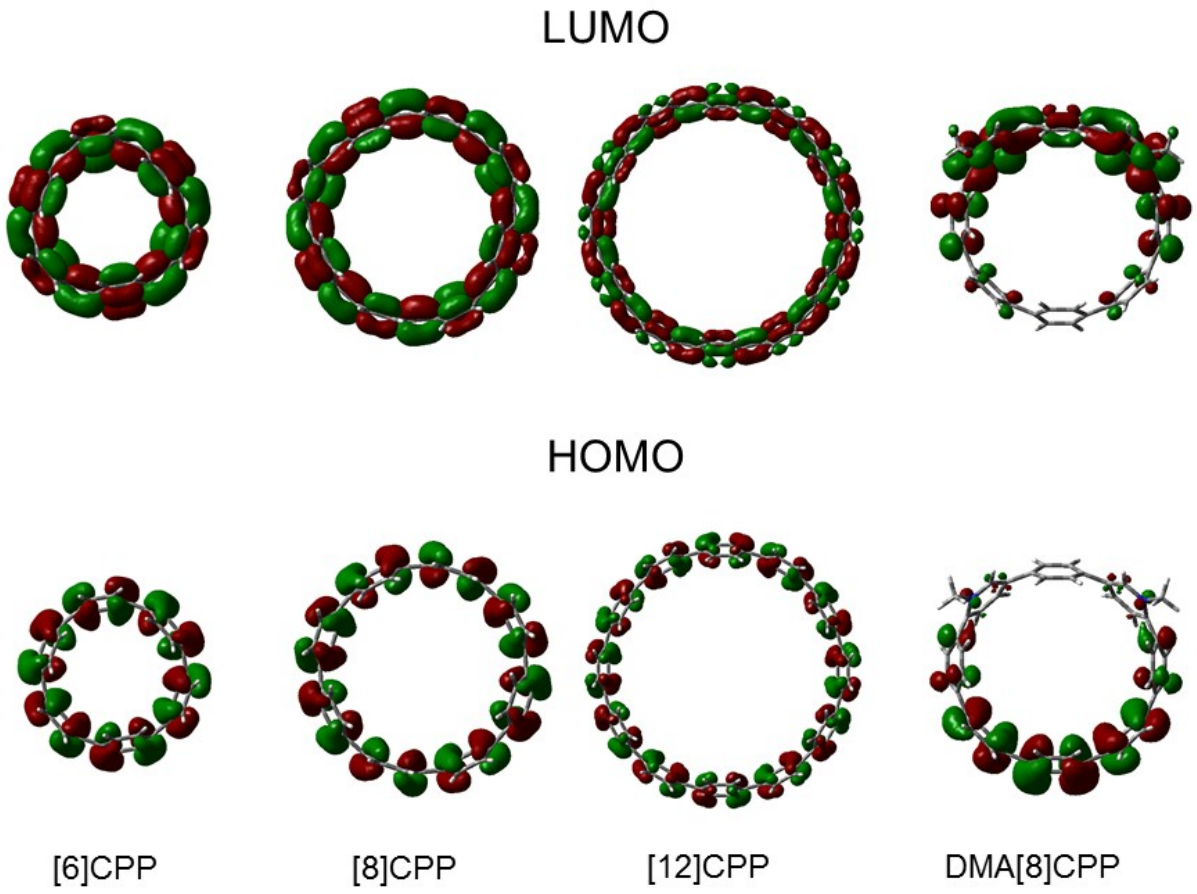

Figure S4. The frontier molecular orbitals of [6]CPP, [8]CPP, [12]CPP and DMA[8]CPP, computed at B3LYP/6-31G* level of theory.

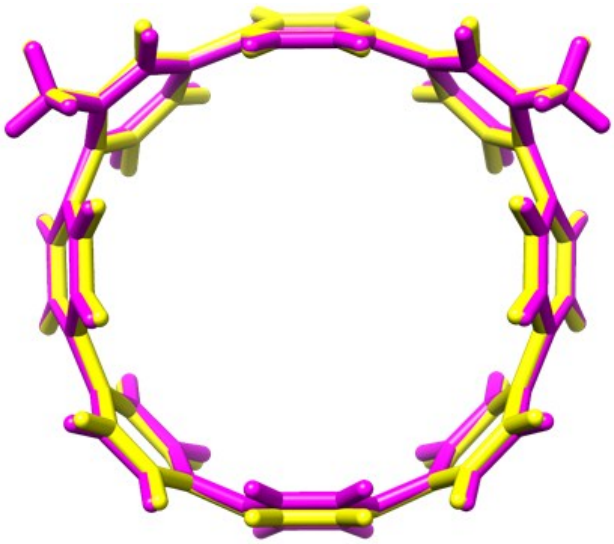

Figure S5. Comparison between the equilibrium structure of the oxidized form (yellow) and the reduced form (magenta) of DMA[8]CPP. From B3LYP/6-31G* calculations in vacuo.

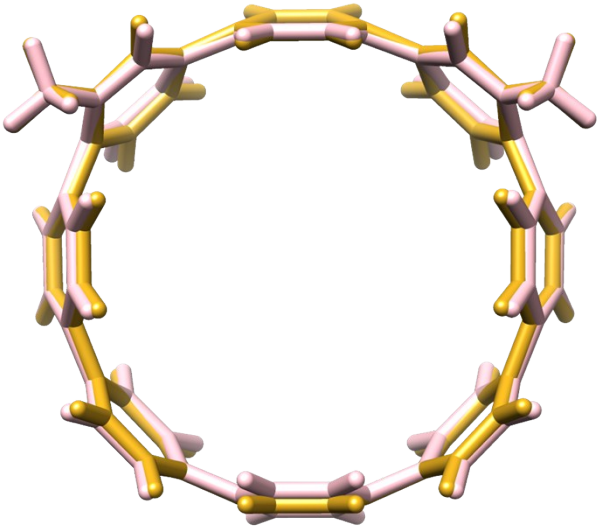

Figure S6. Comparison between the equilibrium structure of the oxidized form (gold) and the reduced form (pink) of DMA[8]CPP. From B3LYP/6-31G* calculations in acetonitrile described with the CPCM model supplemented with intra-molecular dispersion interactions described with the D3(BJ) correction term.

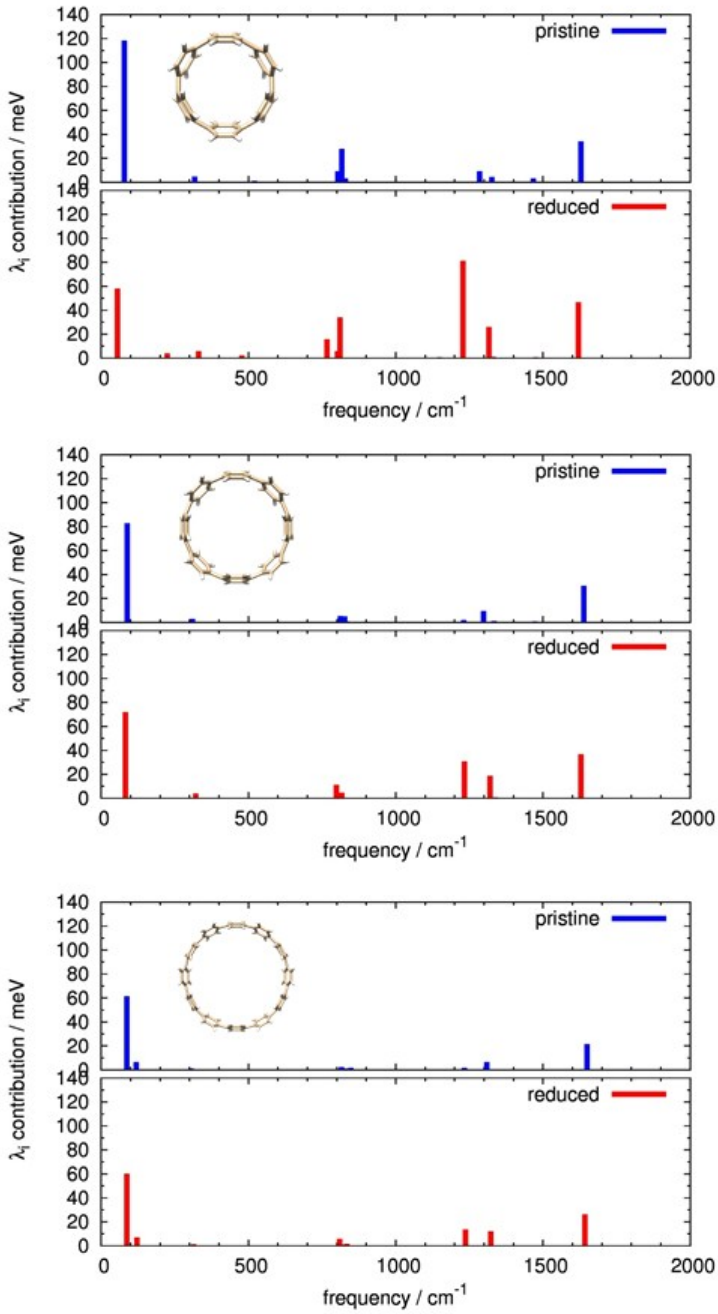

Figure S7. B3LYP/6-31G* calculations of the vibrational frequency contributions (from HR factors) to the computed intramolecular reorganization energies (for *n*-type charge transport) of [6]CPP (top), [8]CPP (middle) and [12]CPP (bottom). Each graph shows the contribution from pristine species on the top and from the reduced species in the bottom part.

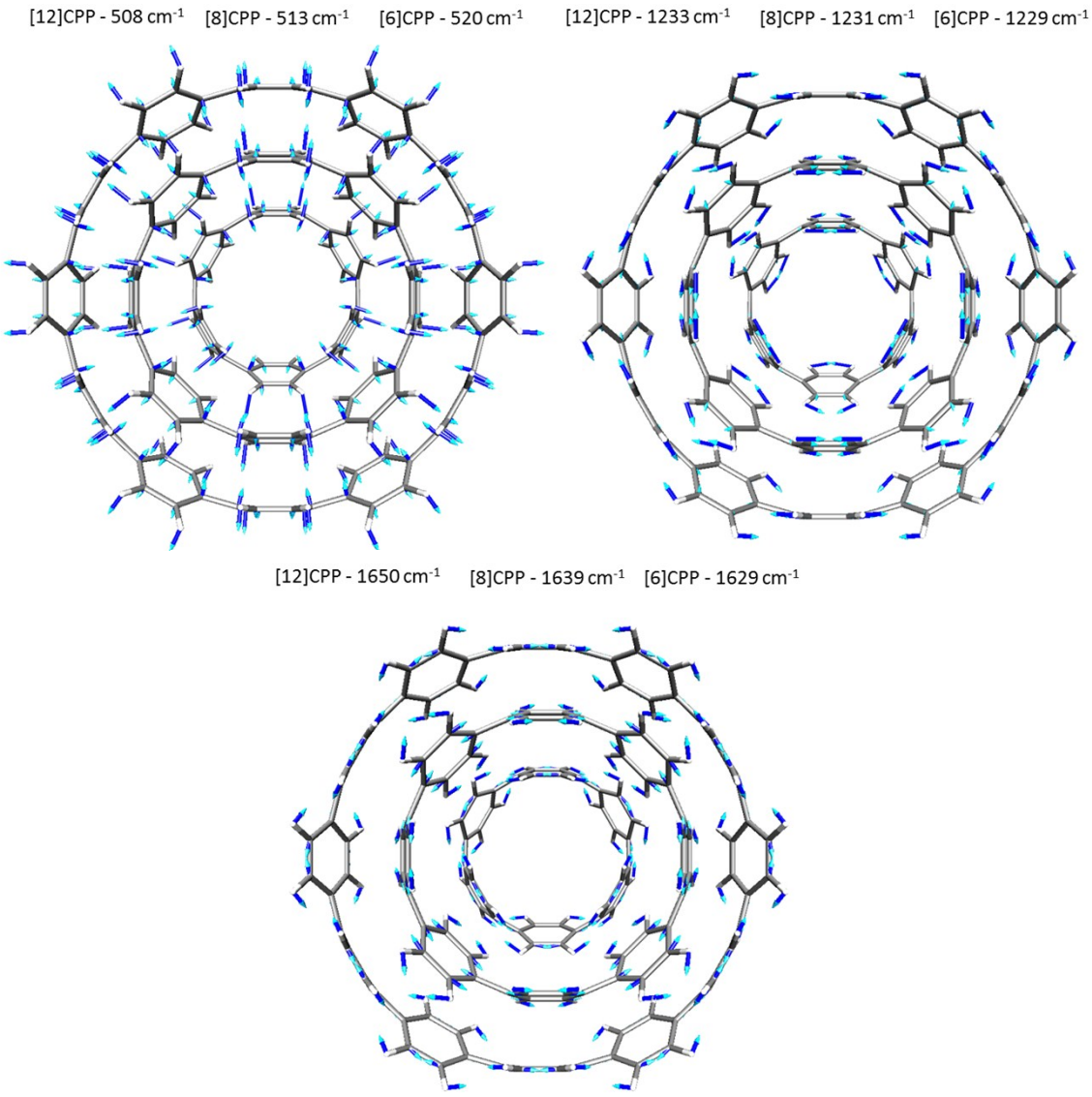

Figure S8. Graphical representation of the medium-high frequency vibrational normal modes contributing to the reorganization energy of the [n]CPP series. From outside to inside [12]CPP, [8]CPP and [6]CPP. From B3LYP/6-31G* calculations. The three structures are not in the same scale. They were rescaled to fit one inside the other.

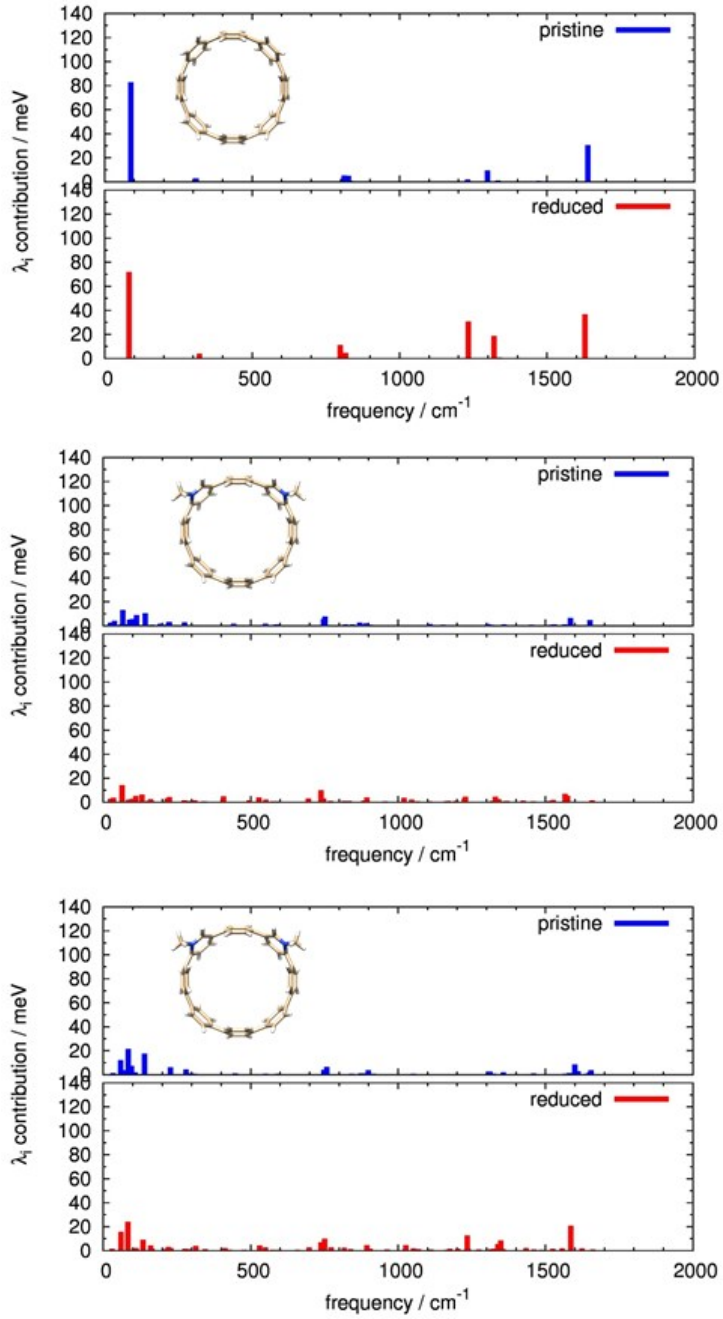

Figure S9. B3LYP/6-31G* calculations of the vibrational frequency contributions (from HR factors) to the computed intramolecular reorganization energies (for *n*-type charge transport) of [8]CPP (top), DMA[8]CPP in vacuo (middle) and DMA[8]CPP in acetonitrile solvent (CPCM) plus dispersion interactions described with the D3(BJ) correction term (bottom). Each graph shows the contribution from pristine species on the top and from the reduced species in the bottom part.

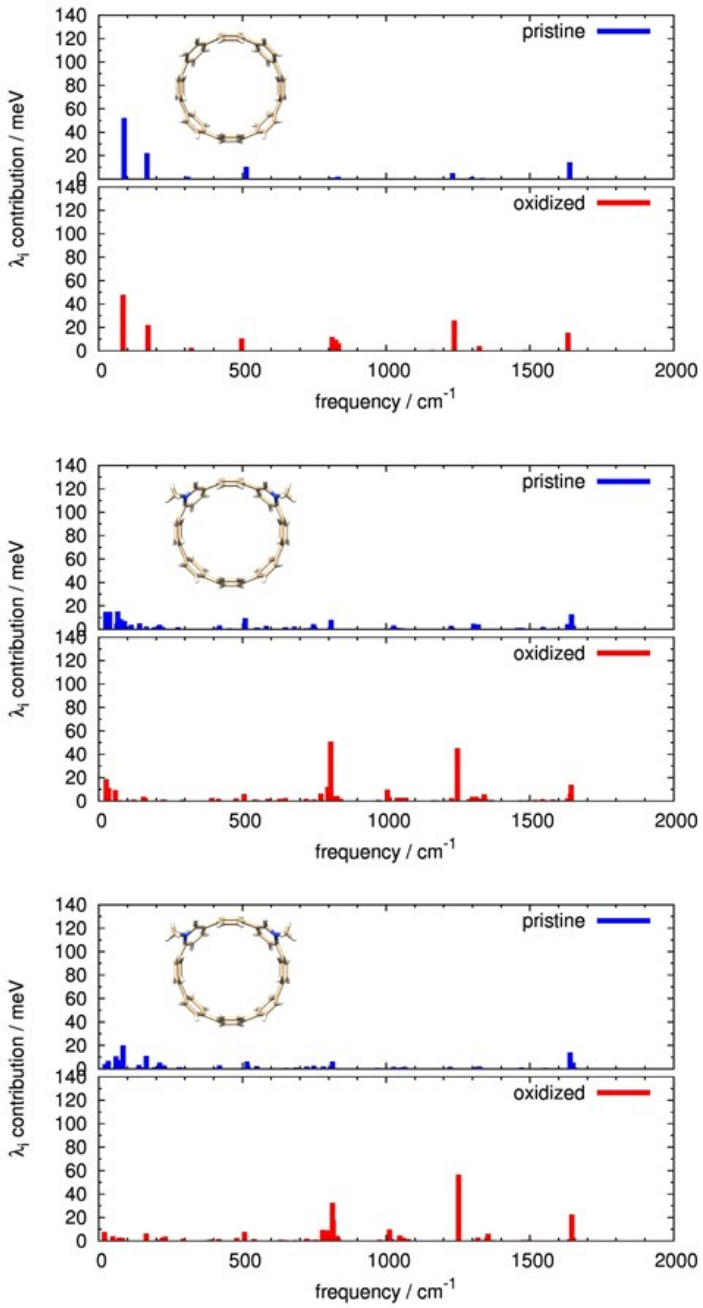

Figure S10. B3LYP/6-31G* calculations of the vibrational frequency contributions (from HR factors) to the computed intramolecular reorganization energies (for *n*-type charge transport) of [8]CPP (top), DMA[8]CPP in vacuo (middle) and DMA[8]CPP in acetonitrile solvent (CPCM) plus dispersion interactions described with the D3(BJ) correction term (bottom). Each graph shows the contribution from pristine species on the top and from the reduced species in the bottom part.

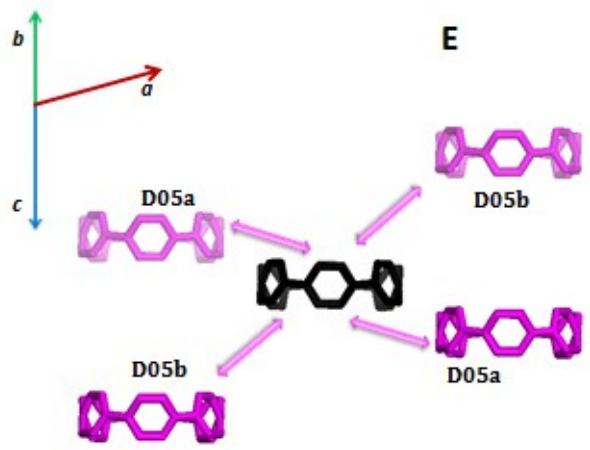

Figure S11. Charge transport paths for the crystal of [6]CPP. Detailed view of path D05 from the central black molecule. Hydrogen atoms omitted for clarity.

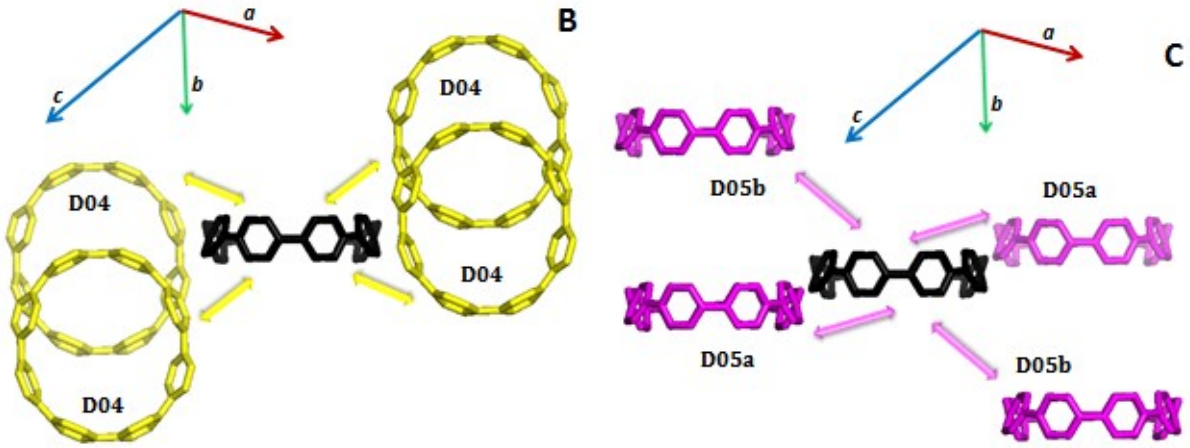

Figure S12. Charge transport paths for the crystal of [8]CPP. Detailed view of paths D04 and D05. (B) Only the paths D04 from the black central nanohoop are shown; (C) only the paths D05 from the black central nanohoop are shown. Hydrogen atoms omitted for clarity.

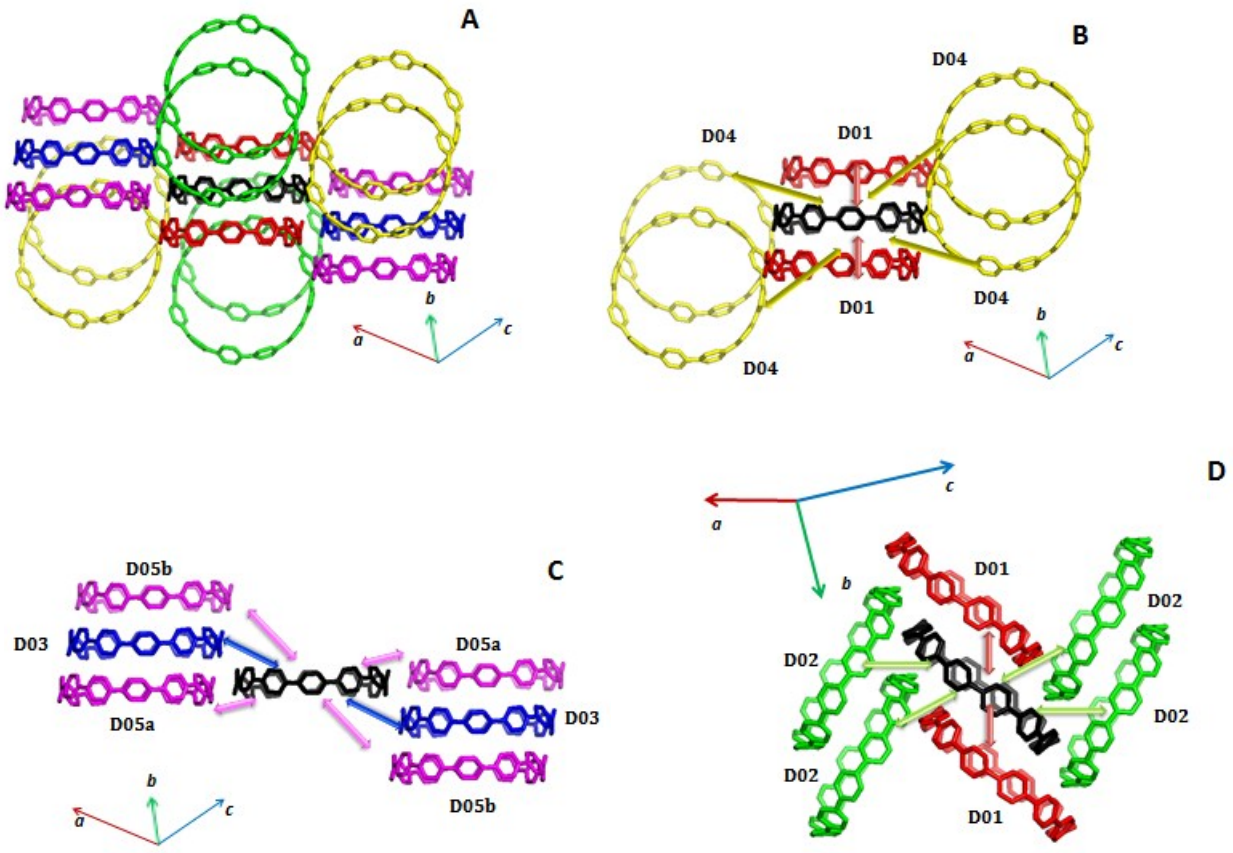

Figure S13. Charge transport paths for the crystal of [12]CPP. (A) View of all the neighbors of the central black molecule considered in calculations. (B) Same as A but with fewer molecules to show the available charge paths D01 and D04 from the black central ring; (C) same as A but with fewer molecules to show the available charge paths D03 and D05 from the black central ring; (D) view of the molecules belonging to central herring bones layer and charge paths D01 and D02 indicated by arrows. Hydrogen atoms omitted for clarity.

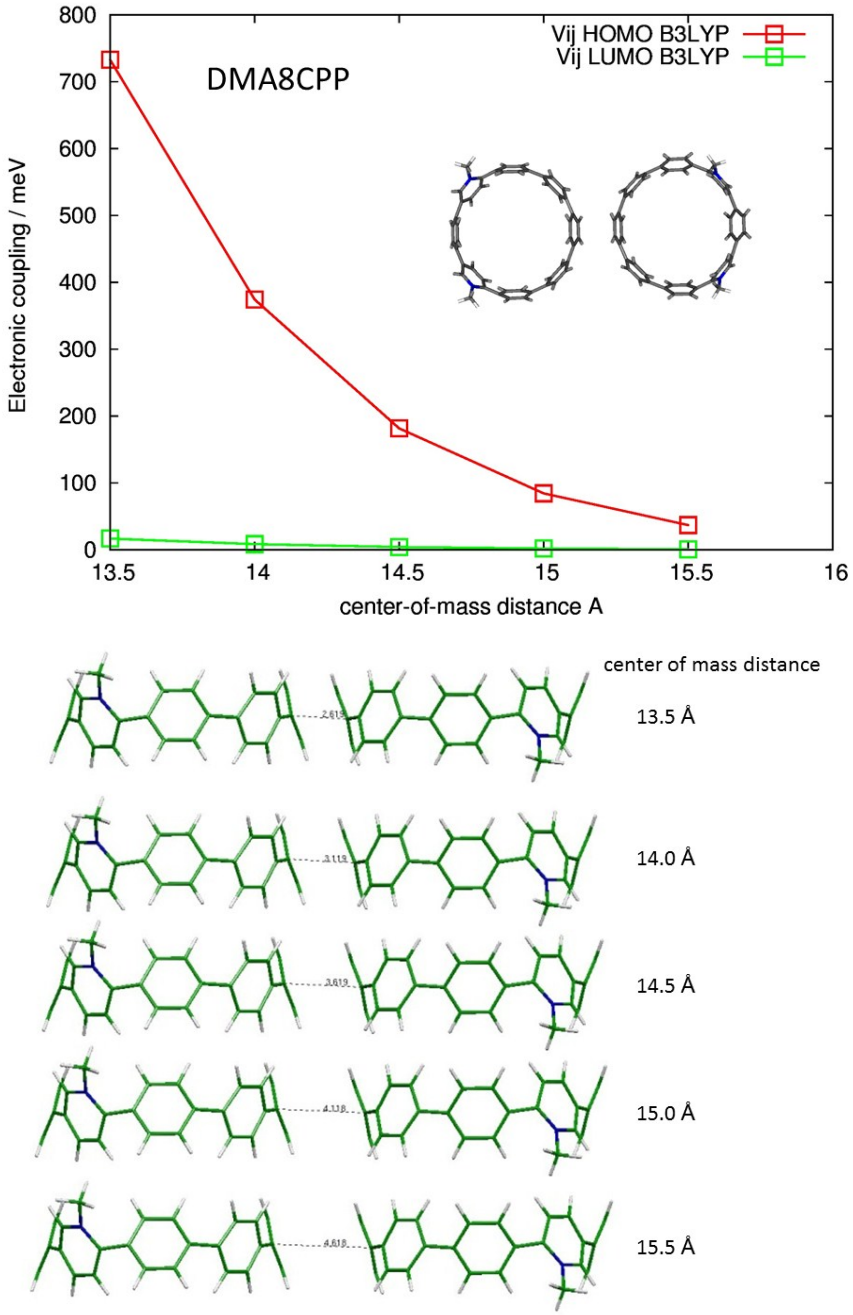

Figure S14. Electronic couplings computed for a model dimer of DMA[8]CPP upon translation of one molecule with respect to the other, showing the modulation of couplings for a configuration of the two molecules favoring ***p*-type interaction**. (top) Electronic couplings computed at B3LYP/6-31G* level, as a function of the distance between centers of mass of the two molecules. (bottom) Graphical representation of the dimers considered in the calculations with the center of mass distance and the distance between the two faced phenyl rings.

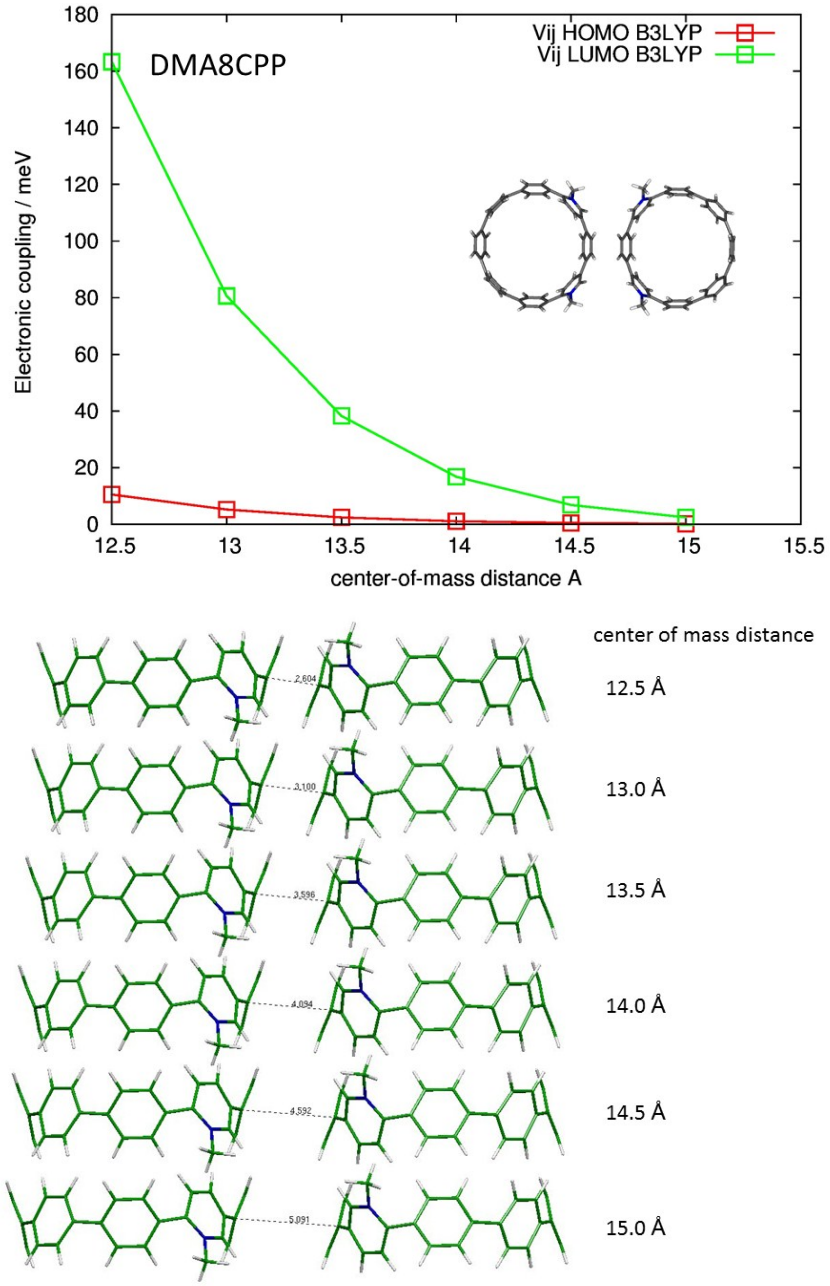

Figure S15 Electronic couplings computed for a model dimer of DMA[8]CPP upon translation of one molecule with respect to the other, showing the modulation of couplings for a configuration of the two molecules favoring **n-type interaction**. (top) Electronic couplings computed at B3LYP/6-31G* level, as a function of the distance between centers of mass of the two molecules. (bottom) Graphical representation of the dimers considered in the calculations with the center of mass distance and the distance between the two faced phenyl rings.

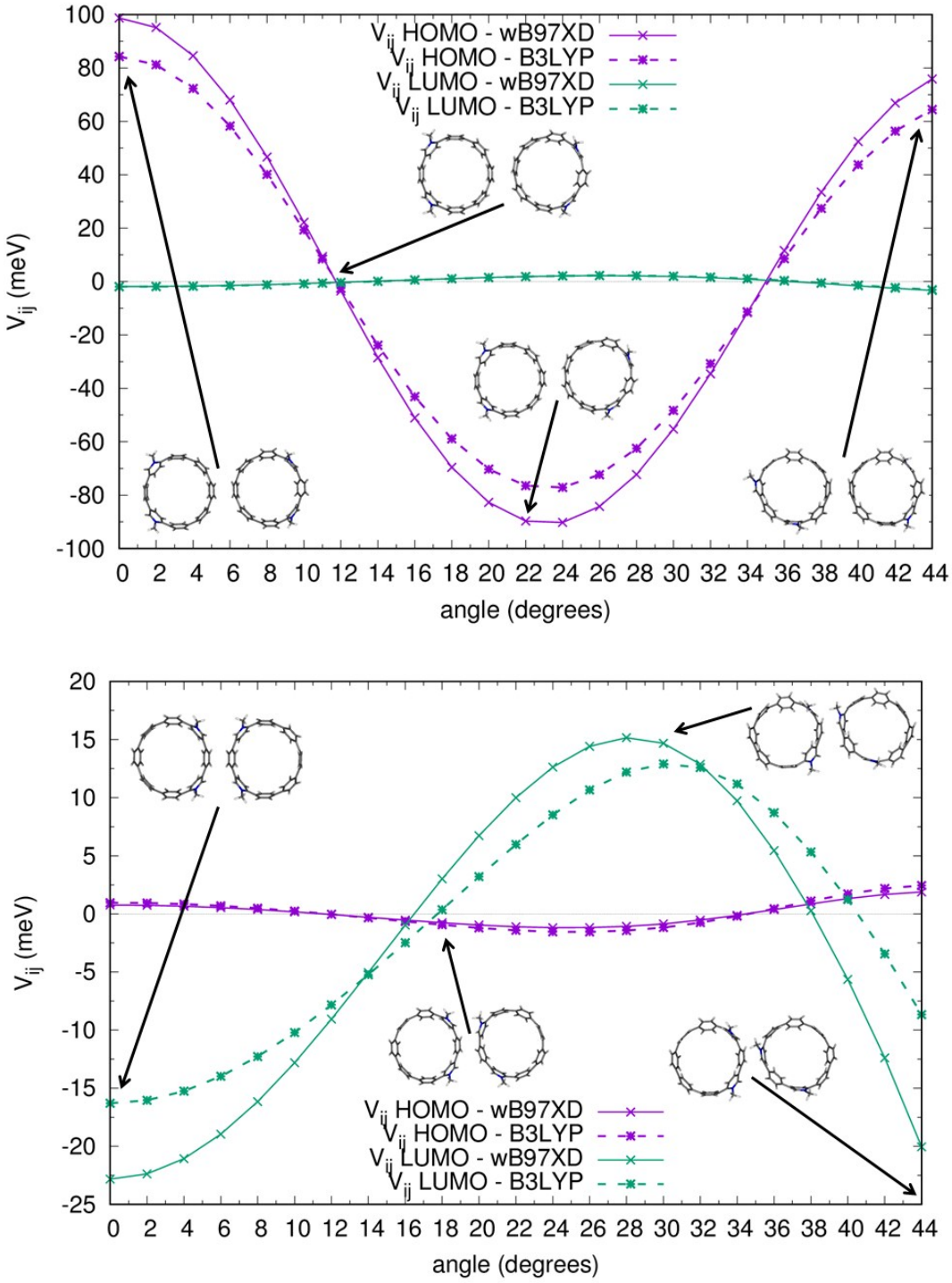

Figure S16. Electronic couplings computed for a model dimer of DMA[8]CPP upon rotation of one molecule with respect to the other, showing the modulation of couplings. (top) Configuration favoring *p*-type interaction, (bottom) configuration favoring *n*-type interaction. Both B3LYP/6-31G* and ωB97XD/6-31G* results are reported.

REFERENCE

(1) Sancho-García, J. C.; Moral, M.; Perez-Jimenez, A. J. Effect of Cyclic Topology on Charge-Transfer Properties of Organic Molecular Semiconductors: The Case of Cycloparaphenylene Molecules. *J. Phys. Chem. C* **2016**, *120*, 9104-9111.